Chemistry & Biology
Article

Deciphering the Molecular Details for the Binding of the Prion Protein to Main Ganglioside GM1 of Neuronal Membranes

Narinder Sanghera,[1] Bruno E.F.S. Correia,[1] Joana R.S. Correia,[1] Christian Ludwig,[2] Sonya Agarwal,[3] Hironori K. Nakamura,[4] Kazuo Kuwata,[4] Eric Samain,[5] Andrew C. Gill,[3] Boyan B. Bonev,[6] and Teresa J.T. Pinheiro[1,*]
[1]School of Life Sciences, University of Warwick, Gibbet Hill Road, Coventry CV4 7AL, UK
[2]HWB-NMR, CR UK Institute for Cancer Studies, University of Birmingham, Vincent Drive, Edgbaston, B15 2TT, UK
[3]Neuropathogenesis Division, Roslin Institute and R(D)SVS, University of Edinburgh, Easter Bush, Roslin, Midlothian EH25 9RG, UK
[4]Center for Emerging Infectious Diseases, Gifu University, 1-1, Yanagido, Gifu 501-1194, Japan
[5]Centre de Recherches sur les Macromolécules Végétales (CERMAV–CNRS), affiliated with Joseph Fourier University and member of the ICMG (Institut de Chimie Moléculaire de Grenoble), BP 53, 38041 Grenoble Cedex 9, France
[6]School of Biomedical Sciences, University of Nottingham, Queen's Medical Centre, Nottingham NG7 2UH, UK
*Correspondence: t.pinheiro@warwick.ac.uk
DOI 10.1016/j.chembiol.2011.08.016

SUMMARY

The prion protein (PrP) resides in lipid rafts in vivo, and lipids modulate misfolding of the protein to infectious isoforms. Here we demonstrate that binding of recombinant PrP to model raft membranes requires the presence of ganglioside GM1. A combination of liquid- and solid-state NMR revealed the binding sites of PrP to the saccharide head group of GM1. The binding epitope for GM1 was mapped to the folded C-terminal domain of PrP, and docking simulations identified key residues in the C-terminal region of helix C and the loop between strand S2 and helix B. Crucially, this region of PrP is linked to prion resistance in vivo, and structural changes caused by lipid binding in this region may explain the requirement for lipids in the generation of infectious prions in vitro.

INTRODUCTION

Prion diseases are fatal neurological disorders characterized by the structural conversion of the normal, α-helical, cellular prion protein (PrP^C) to a β sheet-rich aggregated state. PrP^C is a glycosylphosphatidylinositol (GPI)-anchored membrane protein expressed predominantly in the brain (Stahl et al., 1987). Like most GPI-anchored proteins, PrP is trafficked into specialized lipid raft domains that are rich in cholesterol and sphingolipids (Vey et al., 1996). Numerous roles have been ascribed to lipid rafts, and these roles include organization and compartmentalization of signaling molecules. Lipid rafts have also been suggested to provide vehicles for endocytosis and trafficking of signaling components to and from the cell membrane. The emerging view of cellular membranes and signaling mechanisms indicates that the signaling molecules are arranged in stable and sometimes preformed complexes at the cell surface (Allen et al., 2007). The study of protein interactions with their natural cellular neighbors, be it other proteins, lipids, or carbohydrates, is important to identify those associations relevant for their normal function and, in the case of the prion protein, may also shed some light on the disease mechanism. In this context, the study of PrP-lipid interactions is of particular interest, since lipids are also one of the few constituents that appear necessary to allow the generation of infectious prions in vitro (Deleault et al., 2007; Wang et al., 2010).

In a recent study, we have shown that the majority of PrP in neuronal cell lines is found at the cell surface in lipid raft domains rich in ganglioside GM1 (Sanghera et al., 2008). Gangliosides are a family of glycosphingolipids that are abundant in the brain, representing up to 10% of a neuron's total lipid content, and are a major component of lipid rafts (Ledeen, 1978). These molecules appear to play a crucial role in neuronal differentiation and function (Ferrari and Greene, 1998; Ledeen et al., 1998). In addition, gangliosides such as GM1 promote neuroregeneration when added exogenously to damaged neurons, which has led to the investigation of the therapeutic potential of these compounds in neurological disorders (Mocchetti, 2005). Gangliosides may also play a more direct role in neurological diseases. For example, GM1-gangliosidosis is a lysosomal storage disease that is characterized by the accumulation of GM1 in the brain and the formation of membranous cytoplasmic bodies in neurons (Tessitore et al., 2004). In Alzheimer's disease, the concentration of GM1 in the cerebrospinal fluid of patients is significantly higher compared to aged-matched controls, leading to the proposal that gangliosides including GM1 are involved in disease pathogenesis (Blennow et al., 1991). In the present study, we describe the binding of full-length, recombinant prion protein, PrP(23–231), to lipid systems, including model raft membranes. We have identified a specific interaction with GM1, the main ganglioside in neuronal membranes, and have employed a comprehensive range of spectroscopic analyses to characterize this interaction. We present a molecular model of the PrP-GM1 interaction, and the likely location of the binding of GM1 on PrP points to a role for the complex in modulating prion protein misfolding.

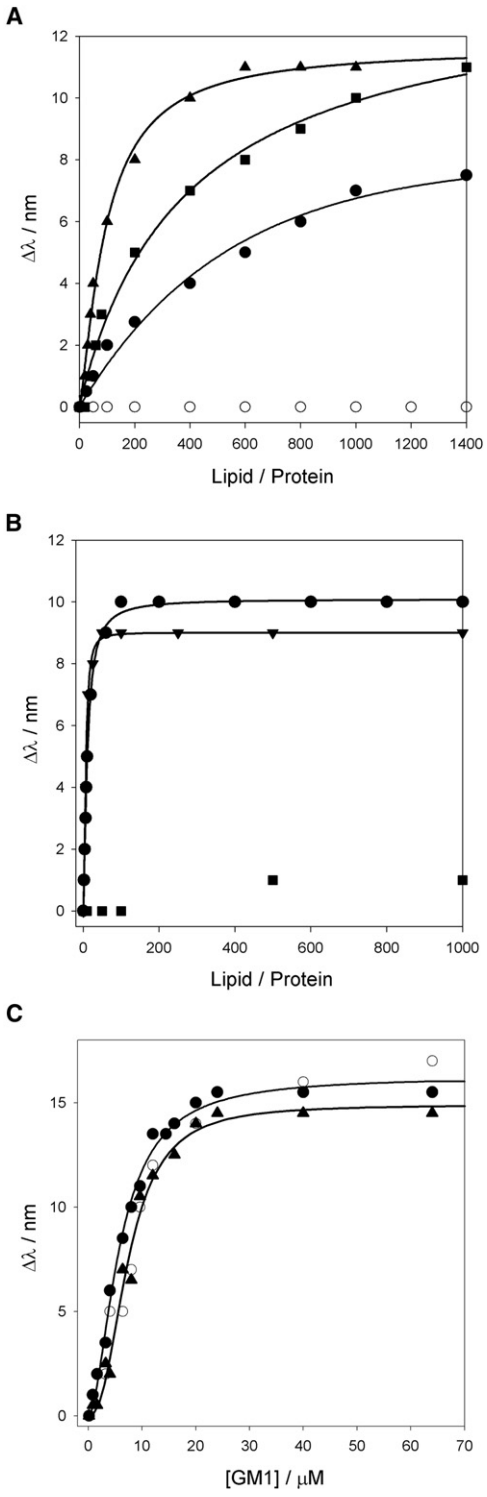

Figure 1. Binding of PrP(23–231) to Different Lipids. The blue shift (Δλ) of the fluorescence maximum for PrP(23–231) in the presence of lipid membranes relative to PrP(23–231) in solution

(A) Binding of PrP(23–231) to model raft membranes composed of DPPC, cholesterol (chol), and sphingomyelin (SM) (molar ratio of 5:3:2) at pH 5 (open circles) and GM1-enriched rafts containing DPPC/chol/SM/GM1 (molar ratio 10:6:4:5) at pH 7 (triangles), at pH 5 (squares), and in the presence of 200 mM NaCl at pH 5 (filled circles).

(B) Binding of PrP(23–231) to single lipid membranes of POPG at pH 5 (circles) and pH 7 (triangles) and POPC at pH 7 (squares).

(C) Binding of PrP(23–231) to GM1 micelles at pH 7 (filled circles) and with added 200 mM NaCl at pH 7 (open circles) and pH 5 (triangles).

Table 1. Apparent Dissociation Constant (K_{Dapp}) of PrP(23–231) and Truncated Domain PrP(90–231) to GM1 in Vesicles or Micelles and to GM1os

Lipid System	PrP(23–231) K_{Dapp} / μM	PrP(90–231)
GM1-raft vesicles,[a] pH 5	368 ± 8	78 ± 5
GM1-raft vesicles, pH 5 and salt[b]	605 ± 77	—
GM1-raft vesicles,[a] pH 7	129 ± 14	92 ± 3
GM1 micelles, pH 5	12 ± 3	3.9 ± 0.8
GM1 micelles, pH 7	8 ± 1	2.5 ± 0.6
GM1os, pH 5	293 ± 15	—
GM1os, pH 7	239 ± 13	—

K_{Dapp} was calculated using a simple two-state binding model.
[a] GM1-enriched rafts containing DPPC/Chol/SM/GM1 at a molar ratio of 10:6:4:5.
[b] GM1-raft vesicles in the presence of 200 mM NaCl.

RESULTS

GM1 Is Required for Binding of PrP(23–231) to Model Raft Membranes

Binding of proteins to lipid vesicles is accompanied by a blue shift of intrinsic tryptophan fluorescence from the protein (Kazlauskaite et al., 2003, Sanghera and Pinheiro, 2002, Schroeder et al., 1994). Here, we use this property to investigate the binding of full length prion protein, PrP(23–231), to model lipid membranes. Studies were undertaken at pH 7 and 5, to model the environment of the plasma membrane and in endosomes, respectively, two subcellular compartments that are involved in the normal cell biology of PrP^C and are also implicated in prion pathogenesis (Borchelt et al., 1992; Caughey and Raymond, 1991; Caughey et al., 1991). The fluorescence spectra of PrP(23–231) in solution at pH 5 and 7 have a maximum intensity at 350 nm (λ_{max}), which indicates that the Trp residues are predominately solvent exposed. The binding of PrP(23–231) to model raft membranes composed of 1,2-dipalmitoyl-sn-glycero-3-phosphocholine (DPPC), cholesterol, and sphingomyelin (DPPC/chol/SM) with and without GM1 was investigated. We observed binding of PrP(23–231) to model raft membranes enriched with GM1, and this binding resulted in a maximum shift in the λ_{max} of 11 nm (Figure 1A), similar to that observed upon binding of PrP(23–231) to anionic 1-palmitoyl-2-oleoyl-*sn*-glycero-3-phospho-rac-(1-glycerol) (POPG) membranes (Figure 1B). No significant binding was noted with model raft membranes lacking GM1 at either pH 7 (data not shown) or 5 (Figure 1A) or with zwitterionic lipid membranes of 1-palmitoyl-2-oleoyl-*sn*-glycero-3-phosphocholine (POPC) (Figure 1B). Binding of PrP(23–231) to GM1-enriched model raft membranes was reduced in the presence of 200 mM NaCl (Figure 1A), from an apparent dissociation constant K_{Dapp} of 368 ± 8 μM without salt to 605 ± 77 μM in the presence of NaCl (Table 1). Collectively, these results show that the binding of PrP(23–231) to model

raft membranes requires the presence of GM1 lipid and that only part of this interaction is electrostatic.

GM1 micelles were employed to investigate further the interaction between PrP(23–231) and GM1, which revealed a similar binding to GM1 in vesicles with a maximum blue shift of ~15 nm (Figure 1C). Measurements in the presence of 200 mM NaCl resulted in an analogous binding curve (Figure 1C); incremental addition of NaCl (up to 2.2 M) to PrP(23–231)-GM1 complexes at binding saturation did not cause a shift in the λ_{max} of fluorescence from the 335 nm characteristic of the bound state (data not shown). These results indicate that PrP(23–231) is not released from GM1 micelles upon addition of salt, suggesting that the nature of the PrP(23–231)-GM1 interaction is not purely electrostatic.

Lipid binding curves were analyzed with a simple two-state model, and apparent dissociation constants (K_{Dapp}) for PrP(23–231) binding to various lipid systems were compared with those for the N-terminally truncated protein, PrP(90–231), where available (Table 1). The K_{Dapp} values show enhanced binding of N-terminally truncated protein to GM1, either in vesicles or micelles, compared to full-length prion protein, PrP(23–231). The binding of both proteins is stronger with micelles compared with vesicles, and PrP(23–231) shows higher pH dependence, having lower dissociation constants at neutral pH than at pH 5. In contrast, the dissociation constant for PrP(90–231) does not show a significant variation between pH 7 and 5.

Binding of GM1 to PrP(23–231) Induces Subtle Structural Changes in the Protein

The structure of PrP(23–231) bound to GM1 micelles was probed by circular dichroism (CD) and Fourier transform infrared (FTIR) spectroscopy. The broad amide I band in the FTIR spectra of PrP(23–231) in solution was centered around 1660 cm^{-1}, indicating the presence of α-helical structure (Figure 2A). The CD spectrum also shows typical features of a protein containing a large amount of α-helical structure with well-defined minima at 208 and 222 nm (Figure 2B). Both CD and FTIR spectra of PrP(23–231) were found to be identical at pH 5 and 7. The CD spectrum of PrP bound to GM1 micelles shows a small decrease in signal intensity at 222 nm and a more pronounced decrease in intensity at 208 nm. These changes are consistent with a reduction in the amount of random coil structure in the protein rather than loss of α-helical structure. By comparison, the CD spectrum of PrP(23–231) bound to POPG membranes shows a single broad band around 220 nm, clearly indicating that the protein underwent a significant structural rearrangement to β sheet structure caused by POPG. The FTIR spectrum of PrP bound to GM1 micelles shows a broad amide I band centered around 1660 cm^{-1}, indicating the presence of α-helical structure; and the appearance of a shoulder at 1630 cm^{-1} suggests the additional presence of more-ordered, β sheet structure (Figure 2A). In contrast, the amide I band in the FTIR spectra for PrP(23–231) associated with POPG vesicles shows a broad band centered around 1650 cm^{-1} with a well-defined shoulder around 1630 cm^{-1}, indicating the presence of β sheet structure (Figure 2A). As anticipated from the fluorescence binding data, POPC alone does not induce any measurable changes in the protein CD spectrum (data not shown). In summary, the interaction of PrP(23–231) with POPG dramatically alters the structure of the protein to a β-sheet-containing conformation, whereas the interaction with GM1 produces more-subtle changes in the structure of PrP(23–231), consistent with retention of the folded α-helical C-terminal domain and increased structural definition of the unstructured N-terminal tail of PrP(23–231).

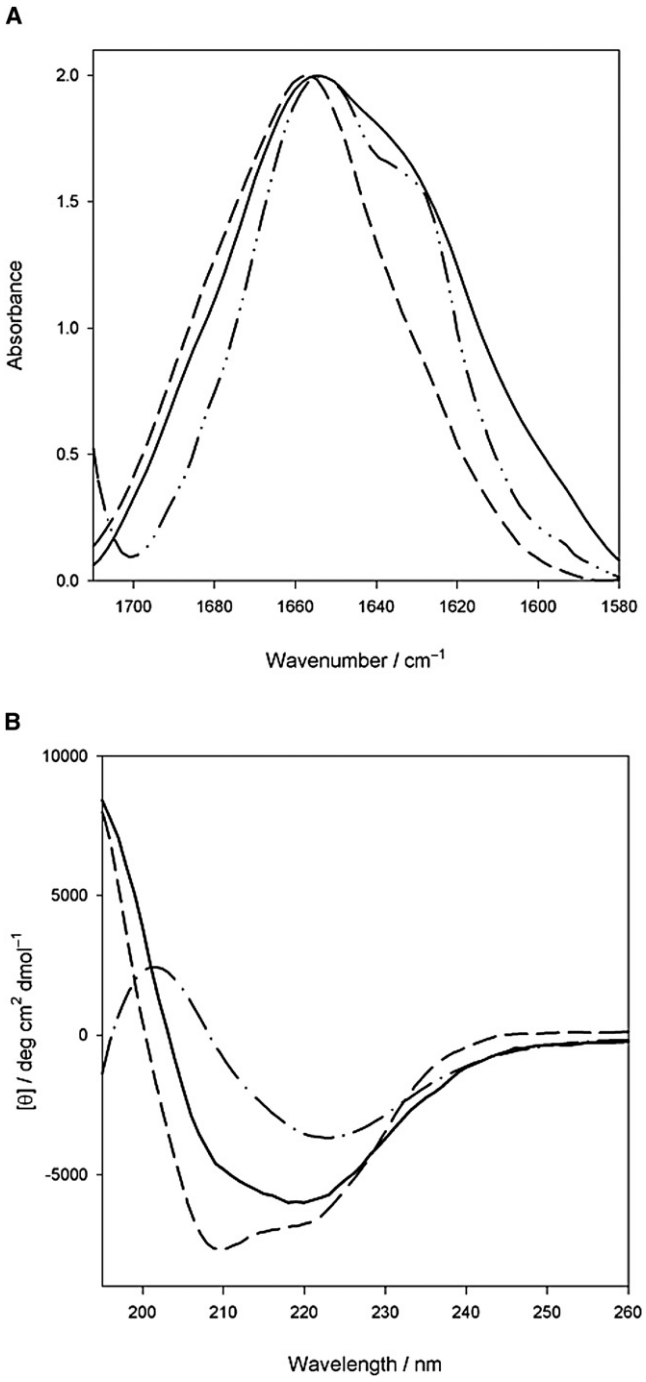

Figure 2. Structural Changes of PrP(23–231) at pH 7.0
(A) Attenuated total reflection Fourier transform infrared and (B) circular dichroism spectra of PrP(23–231) alone (dashed line), with GM1 micelles (continuous line), and with POPG vesicles (dash-dotted line).

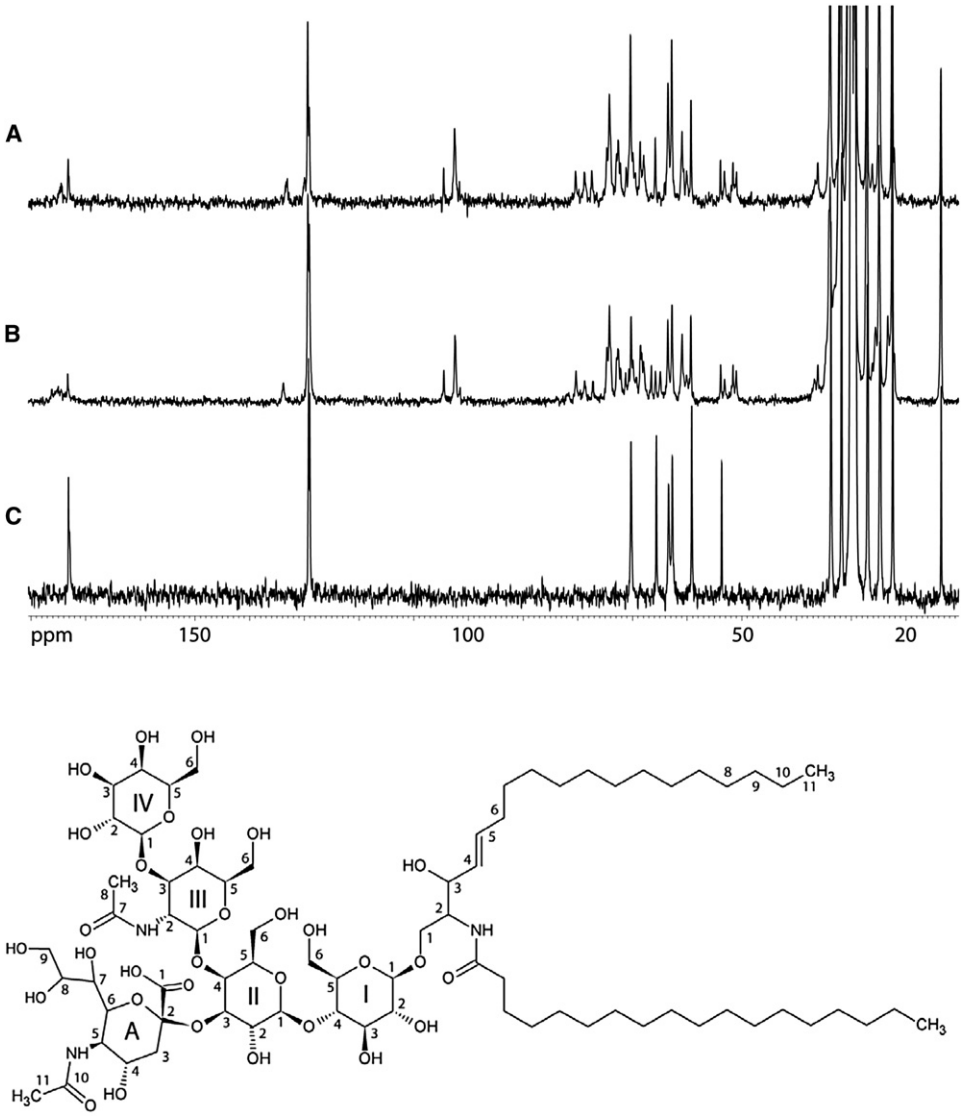

Figure 3. ^{13}C Cross-Polarization/Magic Angle Spinning Solid-State NMR Spectra of Hydrated Lipid Membranes
(A) POPC/GM1 (4:1) with PrP(23–231), (B) POPC/GM1 (4:1), and (C) POPC. The molecular structure shows the carbon numbering scheme for GM1 according to Yagi-Utsumi et al. (2010).

PrP Binds to the GM1 Saccharide Head Group and Inserts into the Lipid Bilayer

The interaction between PrP(23–231) and GM1 in mixed lipid membranes containing POPC/GM1 4:1 was investigated by ^{13}C cross-polarization/magic angle spinning (CP-MAS) solid-state NMR (ssNMR). Spectra with and without PrP(23–231) are shown in Figure 3, and distinct spectral regions are enlarged in Figure 4. Resonances arising from GM1 were assigned by comparison to ^{13}C assignments in solution (Yagi-Utsumi et al., 2010; Pukin et al., 2008). Peaks at low-field (0–40 ppm) arise predominantly from hydrocarbon methylene and methyl groups of both POPC and GM1, as well as from the N-acetyl methyl groups on rings III (C-8, 25.6 ppm) and A (C-11, 22.4 ppm). These resonances (highlighted) are present in the spectrum of GM1/POPC (Figure 4D, middle spectrum) but are absent from the spectrum acquired in the presence of PrP(23–231) (Figure 4D, top spectrum), which is consistent with protein binding to these chemical groups, thereby increasing molecular rigidity and longitudinal relaxation time, T_1. To verify this interpretation, CP-MAS experiments were carried out with the interpulse delay increased from 3.5 to 20 s, which led to marked recovery of signal intensity from the III-8 and A-11 resonances (data not shown).

The majority of GM1 head group resonances fall within spectral region from 50 to 85 ppm (Figure 4C), as do resonances from the sphingosine backbone carbons, C-1 and C-2. Spectral changes on addition of PrP(23–231) include loss of intensity in resonances A-7 (66.6 ppm) and A-9 (65.0 ppm), as well as A-8 (68.3 ppm). An upfield shift in resonance II-4 at the glycosidic bond with ring III, from 77.2 to 77.4 ppm, points to involvement of ring II in the binding epitope. A small downfield shift in A-6

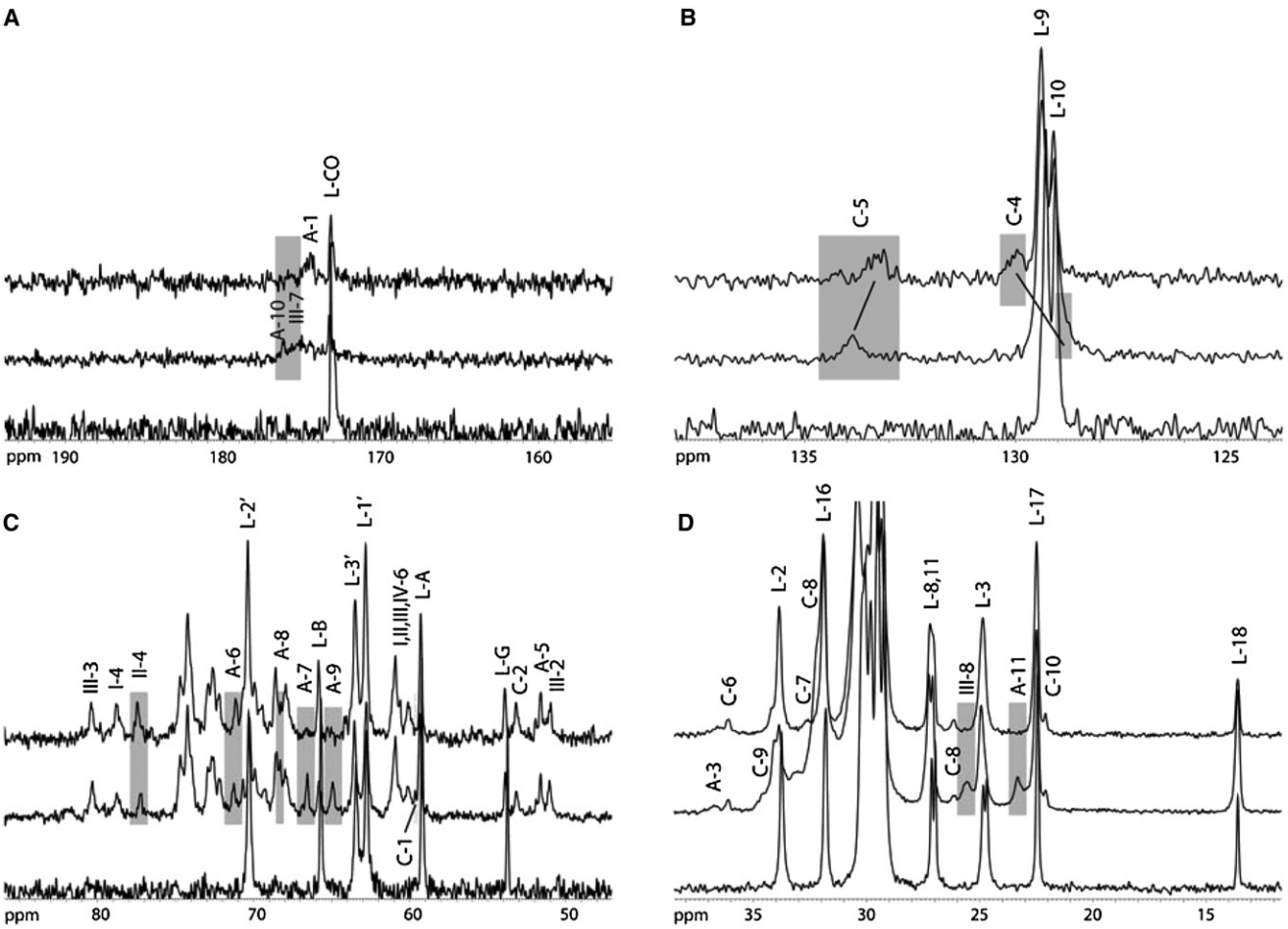

Figure 4. Enlarged Spectral Regions from the ^{13}C Magic Angle Spinning NMR Spectra

The spectra show resonance assignments and highlight changes in spectral intensity and chemical shifts for (A) the carbonyl region, (B) the HC=CH region, (C) the oligosaccharide region, and (D) the hydrocarbon chain and N-acetyl methyl groups for POPC/GM1/PrP(23–231) (top spectrum), POPC/GM1 4:1 (middle spectrum), and POPC (bottom spectrum).

at the base of the propane-triol chain is also observed, from 71.2 to 71.1 ppm. Figure 4A shows the carbonyl spectral region, where signals corresponding to the N-acetyl carbonyls, A-10 and III-7 (175–176 ppm), are lost upon PrP(23–231) binding while the chemical shift and intensity of the A-1 resonance are unaffected. This confirms the involvement of both N-acetyl amino groups in the prion-binding epitope, which appears to comprise the N-acetyl moieties of rings III and A and the propane-triol side chain of ring A and to affect C-4 from ring II. Conversely, the peaks in the spectral region around 100 ppm arise from carbons I-1, II-1, III-1, IV-1, and A-2 and remain relatively unaffected by the binding of PrP(23–231).

A significant shift in resonances of the lipid double bond between C-4 and C-5 suggests insertion of PrP(23–231) into the lipid-water interface. Comparison of the ^{13}C MAS NMR spectra of GM1 (Figure 4B) in the absence (middle spectrum) and in the presence of PrP (top spectrum) shows a downfield shift in C-5 from 133.9 to 133.3 and a concomitant upfield shift in C-4 from 128.9 to 129.9 upon binding of PrP. Furthermore, an increase in spectral intensity of the POPC chain resonances reflects improved CP efficiency and increased order in the lipid chain. Thus, these data show that the saccharide head group of GM1 binds directly to PrP(23–231) and that the protein inserts into the lipid bilayer, stabilizing the lipid chains.

Liquid-State NMR Confirms the PrP Binding Epitope on GM1

To confirm that the binding site of PrP(23–231) to GM1 predicted by ssNMR was the same in solution, we investigated the of binding PrP(23–231) to the GM1 oligosaccharide (GM1os) in solution. Initially, the interaction was followed by fluorescence titration measurements (Figures 5A and 5B). The apparent K_D (Table 1) suggests that PrP(23–231) has weaker affinity for GM1os than for the whole GM1 molecule. In contrast to the binding of PrP(23–231) to GM1, the association of PrP(23–231) with GM1os had no effect on the CD spectrum of the protein (Figure 5C). These data confirm a direct association between PrP and GM1os but suggest that the lipid chains of GM1 are required to mediate structural changes in PrP.

The binding epitope for PrP(23–231) on GM1os was investigated by means of solution-phase NMR. ^{1}H NMR and one-dimensional saturation transfer difference (STD) NMR spectra

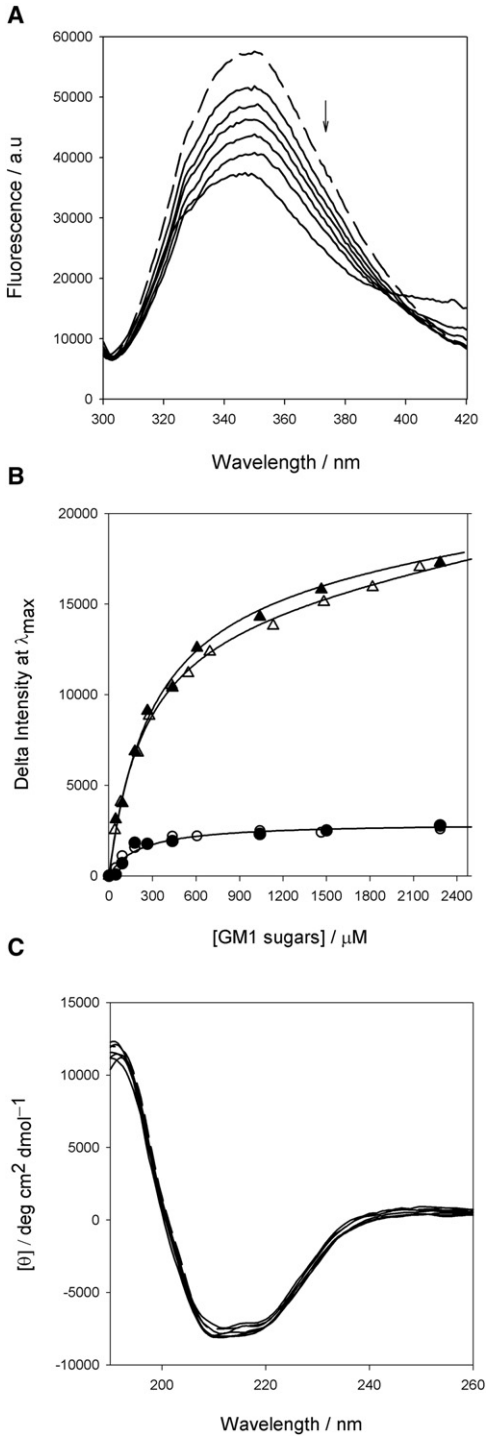

Figure 5. Binding of GM1os to PrP

(A) Typical quenching spectra of PrP(23–231) with increasing concentrations of GM1os (continuous lines; in the direction of the arrow) compared to PrP(23–231) alone (dashed line).

(B) Changes in maximum fluorescence intensity plotted as a function of GM1os concentration for PrP(23–231) (triangles) and PrP(23–110) (circles) at pH 5.0 (filled symbols) and pH 7.0 (open symbols). The data are fitted to a simple two-state model.

(C) Circular dichroism spectra of PrP(23–231) alone at pH 5.0 (dashed line) and with increasing concentrations of GM1os (45 μM to 2 mM; black lines).

of GM1os bound to PrP(23–231) are shown in Figure 6. NMR assignments for protons of GM1os have been reported previously (Ong and Yu, 1986). Protons that interact strongly with the protein binding site produce large signals in the STD-NMR spectra and show that the strongest interaction between GM1os and PrP(23–231) is around ring A, with the largest STD signals along the propane-triol side chain of ring A. The two methyl signals of the N-acetyl groups of ring A and III also indicate of a strong interaction. The NMR data suggest that the binding epitope on GM1os is located in the center of the molecule. Ring A seems to be the most important part of the molecule for the interaction with the protein. These data allowed us to develop a molecular schematic for the recognition of PrP(23–231) as shown in Figure 6C, and the data confirm that the epitope in solution is the same as that determined by ssNMR.

GM1 Binds to PrP(23–231) in the Vicinity of the C Terminus

To identify the GM1os binding sites on the protein, GM1 titration experiments were performed with an N-terminal fragment of PrP comprising amino acids 23–110. Compared to the binding of full-length PrP to GM1os, the binding of the N-terminal domain to GM1os was significantly reduced (Figure 5B), suggesting that the major binding site(s) for GM1 is present on the structured C-terminal domain of the protein. In support of this conclusion, we observed binding of N-terminally truncated protein, PrP(90−231), to all GM1-containing lipid systems studied (Table 1).

Docking simulations were used to investigate the region of PrP to which the GM1 saccharide binds. The docking of GM1os generated a binding site between the C-terminal end of helix C and the loop between β strand S2 and helix B of PrP (Figure 7A), and the proposed model of PrP/GM1 complex is consistent with results from both solution-phase and ssNMR experiments. In our model, Ser222 is located at the center of the binding site (Figure 7D) and may interact with the propane-triol side chain and the carboxyl group of ring A. The propane-triol side chain of ring A inserts into a pocket formed between Ser222 and Asn170, allowing backbone atoms of the loop between strand S2 and helix B to participate in additional hydrogen bonding with the propane-triol group. GM1 hydrogen atoms predicted to be involved in binding by solution-phase NMR are located close to side chain atoms of Val166 or Tyr225. The N-acetyl groups of ring A and ring III are proposed to be located near Asn170 and Gln219, respectively. The docking simulations revealed interactions with rings I and IV of the GM1 saccharide, which STD and ssNMR spectra suggested were not involved in binding to PrP. This may be because docking modes with maximum interactions or the lowest docking energy are always favored. However, molecules fluctuate in the aqueous membrane interface, and although the present model shows interaction between PrP and rings I and IV of GM1os, it may represent a static docking model, which suggests that these regions fluctuate and may not bind tightly to PrP.

DISCUSSION

The association of PrP with membranes appears to play a central role in its biology (Caughey et al., 2009; Pinheiro, 2006). In the

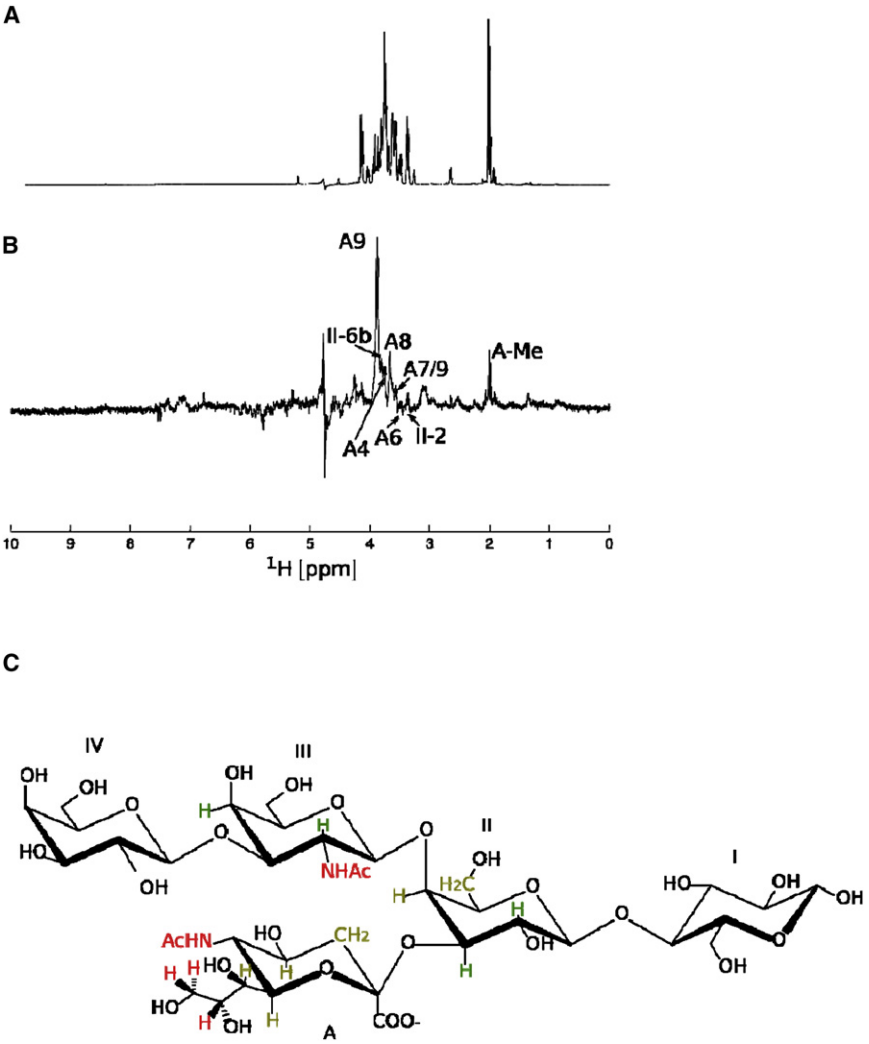

Figure 6. ^{1}H-NMR Spectrum of GM1os in Association with PrP(23–231) at pH 5.0

(A) One-dimensional spectrum of GM1os bound to PrP(23–231) in D_2O showing all resonances.

(B) Saturation transfer difference (STD) NMR spectrum of GM1os bound to PrP(23–231). Protons making close contact with the protein show significant enhancement of their resonances, and the signal intensity is proportional to the strength of binding.

(C) Schematic of GM1os with atoms making contact with the protein highlighted. Weak interactions are marked in green, whereas medium and strong interactions are shown in yellow and red, respectively. Protons showing no interactions in the STD-NMR spectrum are unmarked and/or not plotted.

present study, we report on the binding of full-length prion protein PrP(23–231) to lipid membranes. We show that PrP(23–231) binds with high affinity to anionic lipid membranes but does not interact with zwitterionic membranes (Figure 1B); these properties are similar to the lipid binding properties reported for the truncated protein (Kazlauskaite et al., 2003; Sanghera and Pinheiro, 2002). Our results are consistent with those of other studies of the binding of full-length PrP to anionic membranes (Morillas et al., 1999). In contrast, the binding of PrP(23–231) to model raft membranes, DDPC/chol/SM, is different from that reported for N-terminally truncated PrP. Whereas PrP(90–231) was found to bind to DPPC/chol/SM vesicles at pH 7 but not at pH 5 (Sanghera and Pinheiro, 2002), PrP(23–231) does not bind to these membranes. Binding of full-length PrP to raft membranes was observed only in the presence of GM1 (Figure 1A), suggesting a direct interaction between PrP and GM1.

To decipher the molecular details of the binding of PrP to GM1 lipid, we measured the interaction of PrP(23–231) with GM1 in micelles and lipid bilayers (vesicles) and compared with the binding of the protein to the GM1 oligo saccharide, GM1os. PrP(23−231) binds to GM1 in vesicles or micelles and to GM1os with apparent K_D values in the micromolar range (Table 1), indicating a significant interaction with the saccharide moiety. Considering that PrP(23−231) has a high net positive charge (+9 and +18 at pH 7 and 5, respectively), we anticipated an interaction driven by electrostatic forces between positively charged amino acids and negatively charged groups of GM1. However, no binding was observed between the positively charged N-terminal domain of PrP(23−110) (+10 and +15 at pH 7 and 5, respectively) and GM1os (Figure 5B). Together, these results strongly suggest that the association between PrP and GM1 occurs through a more specific binding than a purely electrostatic interaction. In previous studies, we have shown that binding of PrP(90–231) to negatively charged lipid membranes involves both electrostatic and hydrophobic interactions (Sanghera and Pinheiro, 2002). Since GM1 micelles cannot be dissociated from PrP(23–231) by salt, and competition-binding measurements in the presence of salt had little effect (Figure 1C), hydrophobic forces are clearly involved in the binding of PrP(23–231) to GM1. This interpretation is further supported by the experiments with GM1 in raft membranes, which show binding of PrP(23–231) to GM1 in the presence of 200 mM salt, although binding is weaker than in the absence of salt (Figure 1A, Table 1).

Interestingly, the association of PrP with GM1 results in subtle structural changes to the protein, whereas the association with GM1os does not. The binding sites for PrP on GM1 and GM1os appear the same, since NMR indicates common changes in resonances upon binding of PrP. Instead, there appears to be a role for the lipid chains in modulating the structure of PrP in the complex with GM1. The ssNMR results suggest that the sphingosine moiety at the membrane interface may be critical for this effect (Figure 4B). The broader amide I band in

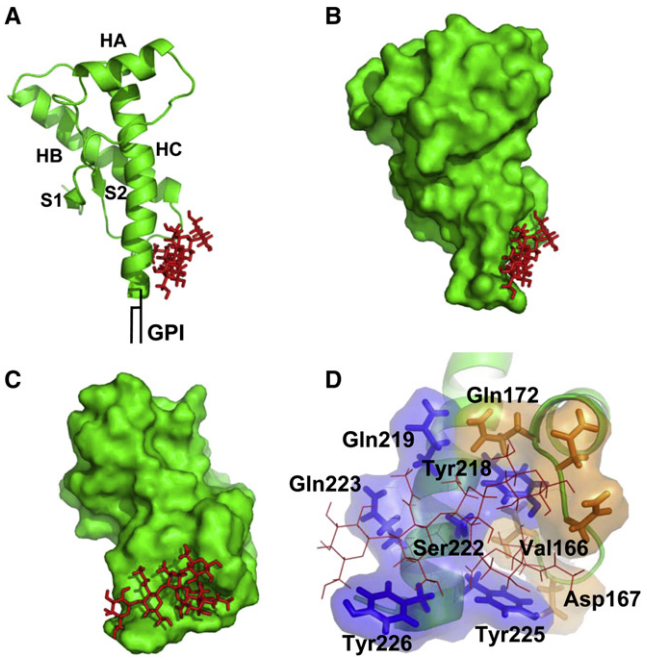

Figure 7. Model of the PrP/GM1os complex

(A) Ribbon diagram of the structure of the PrP globular domain (green) showing α helices HA, HB, and HC and β sheet strands S1 and S2. The location of the glycosylphosphatidylinositol lipid anchor is highlighted schematically in black. GM1os, shown in stick representation (red), binds to the region between the C-terminal end of helix C and the loop between strand S2 and helix B.

(B) Same as (A) but PrP is drawn in surface representation.

(C) Same as (B) but the orientation of this panel is a 90° rotation about the vertical axis of (B).

(D) The putative binding site of GM1os on PrP. The region colored in orange represents the loop region between strand S2 and helix B, and the region in blue represents the C-terminal end of helix C. The thin red line represents GM1os. All panels are rendered by means of PyMOL (DeLano and Lam, 2005).

the FTIR spectrum of PrP associated with GM1 micelles and the change in the CD spectrum (Figure 2) are likely to be associated with ordering of the random coil tail of the protein at the membrane interface. These results are in line with our previous findings, which showed that raft membranes preserve the native α-helical structure of the truncated folded domain of PrP (4). This interpretation is further supported by electron microscopy of PrP bound to vesicles containing GM1, where the protein appears to be smoothly bound to the vesicle surface (data not shown). In stark contrast, the binding of PrP to POPG membranes induces a conformational change to a β sheet structure and promotes the formation of protein aggregates at the membrane surface, similar to the aggregation observed with the truncated protein (Kazlauskaite et al., 2003).

The predicted binding epitope for GM1 on PrP involves the loop region between β strand S2 and α helix B and the C-terminal end of α helix C. This epitope seems reasonable, given the predominant orientation of PrP^C imposed by the tethering to the cell surface via the GPI anchor (Figure 7A). In this orientation, the PrP binding epitope would be accessible to GM1 molecules in the membrane. The proposed binding of GM1os to the loop region between strand S2 and helix B of PrP is especially pertinent since this region strongly influences prion susceptibility (Belt et al., 1995; Westaway et al., 1994). A recent molecular dynamics simulation study analyzed most known disease-linked mutations in the prion protein and revealed that the S2-helix B and helix B-helix C regions are the most affected in terms of structure and stability (Rossetti et al., 2011), supporting their crucial role in prion conversion. The key residue whose position varied as a result of pathogenic mutations was Tyr173 (sheep numbering), and in addition, the presence of arginine instead of glutamine at codon 171 in the S2-helix B loop of sheep prion protein has been shown to confer resistance to scrapie. Although the mechanism by which Arg171 interferes with prion propagation is unknown, our recent in vitro folding study of murine recombinant PrP with the Gln167Arg mutation (equivalent to codon 171 in sheep) showed that the mutant protein is less stable than wild-type protein, suggesting that the stability of PrP-Gln167Arg is not the only factor influencing its disease-resistant property (Robinson and Pinheiro, 2009). Alternatively, the introduction of arginine will increase the number of positive charges in the loop region, which in turn may influence the binding of PrP to stabilizing cofactors at the membrane surface, especially in raft domains. Such molecules may include lipid head groups, and this is currently under further investigation. In any case, the current data greatly expand our knowledge of the molecular features of PrP-lipid binding. Understanding such binding events is of crucial importance in light of recent reports of the de novo creation of infectious prions in vitro. To date, all such studies have involved the use of lipids during the prion protein misfolding process, which suggests that lipids may be critically important molecules in vivo to mediate prion protein misfolding during disease Our findings further highlight that GM1 represents a lipid with which PrP may have regular and prolonged contact. The selective binding of GM1, possibly to one of the key areas of PrP directing susceptibility of individuals to prion disease, may be highly significant.

In summary, we report the selective binding of PrP(23–231) to the major neuronal ganglioside, GM1, and the atomic details of this interaction are revealed by NMR and molecular modeling. The findings are highly pertinent given the colocalization of PrP^C and GM1 in neuronal cells (Mattei et al., 2002, Sanghera et al., 2008). GM1 was found to bind to a region of PrP involved in disease susceptibility. Given the high concentrations of gangliosides in neurons and their localization in rafts (Ledeen, 1978), the association of PrP with GM1 may play a role in modulating disease susceptibility. In addition, the interaction of GM1 with PrP may be relevant to the normal function of the prion protein. Although the function of PrP^C is not yet clear, evidence suggests an involvement in cell signaling and cell recognition processes at the cellular membrane (Aguzzi et al., 2008), where protein segregation into rafts and lipid-protein interactions are important.

SIGNIFICANCE

Important interactions with lipids feature in normal prion protein cell biology, prion disease pathogenesis, and during the misfolding of prion protein to infectious conformations, but the molecular details of lipid-prion interactions have previously not been studied. We provide atomic-level detail of both binding epitopes in the complex formed between

the key neuronal ganglioside, GM1, and the prion protein. We find that the binding epitope of GM1 on PrP involves amino acids close to the C terminus of the protein and in regions previously suggested to modulate prion protein misfolding. Thus, our data suggest a means by which lipid-prion protein interactions on the cell surface can mediate protein function and protein misfolding and hence prion disease pathogenesis. The data also indicate how lipid-prion protein interactions could initiate prion protein misfolding by affecting stability of α helices of PrP, and the molecular details of the lipid-prion protein complex will allow such complexes to be targeted by small-molecule inhibitors. Our data represent a major advance in our understanding of the interaction of prion protein with lipids.

EXPERIMENTAL PROCEDURES

Expression, Purification, and Refolding of PrP

SHa PrP(23–231) was expressed in *E. coli* strain BL21* Rosetta.

The recombinant protein accumulated in inclusion bodies within the cytoplasm. The protocol for the purification of PrP(23–231) was adapted from Bocharova et al. (2005), and full details are given in the Supplemental Experimental Procedures available online.

Preparation of Lipid Vesicles and Micelles

Cholesterol, POPC, POPG, and sphingomyelin were purchased from Avanti Polar Lipids, Inc. (Alabaster, AL). DPPC and GM1 were from Sigma-Aldrich (Dorset, UK). Single lipid vesicles of POPG or POPC and mixtures of lipid components of rafts were prepared as described below. Mixed lipid vesicles containing 1,2-dipalmitoyl-*sn*-glycero-3-phosphocholine (DPPC), cholesterol (chol), and sphingomyelin (SM) at a molar ratio of 5:3:2 represent the chol- and SM-rich domains in the plasma membrane known as rafts and are here referred to as "raft membranes." GM1-enriched raft membranes contain DPPC/chol/SM/GM1 at the molar ratio 10:6:4:5 in a solution of chloroform/methanol 80:20 v/v.

Phospholipids in chloroform solutions were dried under a rotary evaporator or a N_2 flow (depending on sample volume). Mixed lipid membranes were prepared by codissolving the constituent lipids in chloroform or chloroform/methanol, and a lipid film formed as described above. Lipid vesicles were prepared by hydrating the dried lipid or lipid mixture with the required buffer (2 mM MES at pH 7 or 5). After lipid hydration, the resulting multilamellar liposome suspension was sonicated in a bath sonicator until a clear suspension of small unilamellar vesicles was obtained (typically 6 × 1/2 h periods).

Micelles of GM1 were prepared in the required buffers (2 mM MES pH 7 or 5). Typically, a 2 mM GM1 solution was prepared using an aliquot of a stock of GM1 in methanol (6.4 mM). The critical micelle concentration of GM1 is 10^{-8} M (Ohta et al., 2004).

Spectroscopic Measurements

Binding of PrP proteins to vesicles and micelles was studied by fluorescence spectroscopy at both pH 7 and 5 at 20°C by monitoring the shift in λ_{max} of protein fluorescence upon addition of increasing amounts of lipid. All fluorescence spectra were recorded on a Photon Technology International spectrofluorimeter. Attenuated total reflection FTIR spectra were recorded at room temperature on a Vector 22 infrared spectrometer (Bruker) using a germanium internal reflection element as described previously (Kazlauskaite et al., 2003). CD spectra were collected at 20°C using a 0.1 cm path length quartz cuvette (Starna brand, Optiglass Ltd., Hainault, UK) in a Jasco J-715 spectropolarimeter (Jasco, Great Dunmow, UK). Full details of these procedures are given in the Supplementary Experimental Procedures.

Nuclear Magnetic Resonance Spectroscopy

Solution-phase NMR spectra were collected for GM1os/PrP(23–231) complexes containing 0.2 mg PrP(23–231) and a 10-fold excess of GM1os in 5 mM MES pH 5.0 buffer prepared in D_2O. All NMR spectra were acquired on a Varian INOVA 800 MHz spectrometer equipped with a cryogenically cooled HCN probe at 25°C. All ssNMR) experiments were carried out on a Varian 400 MHz VNMRS Direct Drive spectrometer equipped with a 4 mm T3 MAS NMR probe (Varian, Palo Alto, CA). Lipid film containing POPC/GM1 (molar ratio 4:1) was hydrated in 1 ml of MES buffer pH 5.0 and added to 500 μl of PrP(23–231) (200 μg) at pH 5.0. The final lipid/protein ratio was 900:1. Lipid/protein sample was freeze-dried, loaded into a NMR tube, and hydrated. Full details of these procedures are given in the Supplementary Experimental Procedures.

Molecular Modeling of GM1/PrP Complex

Complex structures of GM1os/PrP were generated with docking simulations using AutoDock version 3.05 (Morris et al., 1998). In a first step, docking simulations were performed using virtual mini-GM1s, which share a common substructure with GM1os but lack some functional groups. Using this strategy, it was possible to search a large region, including the overall surface of PrP, for a GM1os binding site. Docking modes obtained by docking simulations were visually inspected to fit to the STD-NMR result. In a second step, we performed docking simulations using an entire GM1os and a restricted search region around a putative binding site identified from the first step. The docking simulations resulted in a number of potential complex structures for PrP/GM1os, from which one complex model was finally selected on the basis of the results of the STD-NMR experiments and the best fit for the docking modes of virtual mini-GM1s. Further optimization for the selected docking model and re-adding hydrogen atoms were performed with Molegro Molecular Viewer (Thomsen and Christensen, 2006). More details of these procedures are given in the Supplementary Experimental Procedures.

SUPPLEMENTAL INFORMATION

Supplemental Information includes Supplemental Experimental Procedures and can be found with this article online at doi:10.1016/j.chembiol.2011.08.016.

ACKNOWLEDGMENTS

We thank Dr. Jurate Kazlauskaite and Dr. Matthew R. Hicks for their early input in planning the experiments and Dr. Sevetla Stoilova-Mcphie for electron microscopy of vesicle/PrP preparations. We acknowledge financial support from BBSRC (grants 88/BS516471 to TJTP and BB/3510924 to BB) and a generous contribution from Varian, Ltd. N.S. and T.J.T.P. designed research; N.S., B.E.F.S.C., J.R.S.C., C.L., S.A., H.K.N., and B.B.B. performed research; ES contributed new reagents; K.K. contributed analytical tools; and N.S., A.C.G., B.B.B., and T.J.T.P. wrote the paper.

Received: June 17, 2011
Revised: August 15, 2011
Accepted: August 16, 2011
Published: November 22, 2011

REFERENCES

Aguzzi, A., Baumann, F., and Bremer, J. (2008). The prion's elusive reason for being. Annu. Rev. Neurosci. *31*, 439–477.

Allen, J.A., Halverson-Tamboli, R.A., and Rasenick, M.M. (2007). Lipid raft microdomains and neurotransmitter signalling. Nat. Rev. Neurosci. *8*, 128–140.

Belt, P.B.G.M., Muileman, I.H., Schreuder, B.E.C., Bos-de Ruijter, J., Gielkens, A.L.J., and Smits, M.A. (1995). Identification of five allelic variants of the sheep PrP gene and their association with natural scrapie. J. Gen. Virol. *76*, 509–517.

Blennow, K., Davidsson, P., Wallin, A., Fredman, P., Gottfries, C.G., Karlsson, I., Månsson, J.E., and Svennerholm, L. (1991). Gangliosides in cerebrospinal fluid in 'probable Alzheimer's disease.' Arch. Neurol. *48*, 1032–1035.

Bocharova, O.V., Breydo, L., Parfenov, A.S., Salnikov, V.V., and Baskakov, I.V. (2005). In vitro conversion of full-length mammalian prion protein produces amyloid form with physical properties of PrP(Sc). J. Mol. Biol. *346*, 645–659.

Borchelt, D.R., Taraboulos, A., and Prusiner, S.B. (1992). Evidence for synthesis of scrapie prion proteins in the endocytic pathway. J. Biol. Chem. *267*, 16188–16199.

Caughey, B., and Raymond, G.J. (1991). The scrapie-associated form of PrP is made from a cell surface precursor that is both protease- and phospholipase-sensitive. J. Biol. Chem. *266*, 18217–18223.

Caughey, B., Baron, G.S., Chesebro, B., and Jeffrey, M. (2009). Getting a grip on prions: oligomers, amyloids, and pathological membrane interactions. Annu. Rev. Biochem. *78*, 177–204.

Caughey, B., Raymond, G.J., Ernst, D., and Race, R.E. (1991). N-terminal truncation of the scrapie-associated form of PrP by lysosomal protease(s): implications regarding the site of conversion of PrP to the protease-resistant state. J. Virol. *65*, 6597–6603.

DeLano, W.L., and Lam, J.W. (2005). PyMOL: A communications tool for computational models. Abstracts of Papers of the American Chemical Society *230*, U1371–U1372.

Deleault, N.R., Harris, B.T., Rees, J.R., and Supattapone, S. (2007). Formation of native prions from minimal components in vitro. Proc. Natl. Acad. Sci. USA *104*, 9741–9746.

Ferrari, G., and Greene, L.A. (1998). Promotion of neuronal survival by GM1 ganglioside. Phenomenology and mechanism of action. Ann. N Y Acad. Sci. *845*, 263–273.

Kazlauskaite, J., Sanghera, N., Sylvester, I., Vénien-Bryan, C., and Pinheiro, T.J.T. (2003). Structural changes of the prion protein in lipid membranes leading to aggregation and fibrillization. Biochemistry *42*, 3295–3304.

Ledeen, R.W. (1978). Ganglioside structures and distribution: are they localized at the nerve ending? J. Supramol. Struct. *8*, 1–17.

Ledeen, R.W., Wu, G., Lu, Z.H., Kozireski-Chuback, D., and Fang, Y. (1998). The role of GM1 and other gangliosides in neuronal differentiation. Overview and new finding. Ann. N Y Acad. Sci. *845*, 161–175.

Mattei, V., Garofalo, T., Misasi, R., Gizzi, C., Mascellino, M.T., Dolo, V., Pontieri, G.M., Sorice, M., and Pavan, A. (2002). Association of cellular prion protein with gangliosides in plasma membrane microdomains of neural and lymphocytic cells. Neurochem. Res. *27*, 743–749.

Mocchetti, I. (2005). Exogenous gangliosides, neuronal plasticity and repair, and the neurotrophins. Cell. Mol. Life Sci. *62*, 2283–2294.

Morillas, M., Swietnicki, W., Gambetti, P., and Surewicz, W.K. (1999). Membrane environment alters the conformational structure of the recombinant human prion protein. J. Biol. Chem. *274*, 36859–36865.

Morris, G.M., Goodsell, D.S., Halliday, R.S., Huey, R., Hart, W.E., Belew, R.K., and Olson, A.J. (1998). Automated docking using a Lamarckian genetic algorithm and an empirical binding free energy function. J. Comput. Chem. *19*, 1639–1662.

Ohta, Y., Yokoyama, S., Sakai, H., and Abe, M. (2004). Membrane properties of binary and ternary systems of ganglioside GM1/dipalmitoylphosphatidylcholine/dioleoylphosphatidylcholine. Colloids Surf. B Biointerfaces *34*, 147–153.

Ong, R.L., and Yu, R.K. (1986). 1H-NMR assignments of GM1-oligosaccharide in deuterated water at 500 MHz by two-dimensional spin-echo J-correlated spectroscopy. Arch. Biochem. Biophys. *245*, 157–166.

Pinheiro, T.J. (2006). The role of rafts in the fibrillization and aggregation of prions. Chem. Phys. Lipids *141*, 66–71.

Pukin, A.V., Weijers, C.A., van Lagen, B., Wechselberger, R., Sun, B., Gilbert, M., Karwaski, M.F., Florack, D.E.A., Jacobs, B.C., Tio-Gillen, A.P., et al. (2008). GM3, GM2 and GM1 mimics designed for biosensing: chemoenzymatic synthesis, target affinities and 900 MHz NMR analysis. Carbohydr. Res. *343*, 636–650.

Robinson, P.J., and Pinheiro, T.J. (2009). The unfolding of the prion protein sheds light on the mechanisms of prion susceptibility and species barrier. Biochemistry *48*, 8551–8558.

Rossetti, G., Cong, X., Caliandro, R., Legname, G., and Carloni, P. (2011). Common structural traits across pathogenic mutants of the human prion protein and their implications for familial prion diseases. J. Mol. Biol. *411*, 700–712.

Sanghera, N., and Pinheiro, T.J. (2002). Binding of prion protein to lipid membranes and implications for prion conversion. J. Mol. Biol. *315*, 1241–1256.

Sanghera, N., Wall, M., Vénien-Bryan, C., and Pinheiro, T.J. (2008). Globular and pre-fibrillar prion aggregates are toxic to neuronal cells and perturb their electrophysiology. Biochim. Biophys. Acta *1784*, 873–881.

Schroeder, R., London, E., and Brown, D. (1994). Interactions between saturated acyl chains confer detergent resistance on lipids and glycosylphosphatidylinositol (GPI)-anchored proteins: GPI-anchored proteins in liposomes and cells show similar behavior. Proc. Natl. Acad. Sci. USA *91*, 12130–12134.

Stahl, N., Borchelt, D.R., Hsiao, K., and Prusiner, S.B. (1987). Scrapie prion protein contains a phosphatidylinositol glycolipid. Cell *51*, 229–240.

Tessitore, A., del P Martin, M., Sano, R., Ma, Y., Mann, L., Ingrassia, A., Laywell, E.D., Steindler, D.A., Hendershot, L.M., and d'Azzo, A. (2004). GM1-ganglioside-mediated activation of the unfolded protein response causes neuronal death in a neurodegenerative gangliosidosis. Mol. Cell *15*, 753–766.

Thomsen, R., and Christensen, M.H. (2006). MolDock: a new technique for high-accuracy molecular docking. J. Med. Chem. *49*, 3315–3321.

Vey, M., Pilkuhn, S., Wille, H., Nixon, R., DeArmond, S.J., Smart, E.J., Anderson, R.G., Taraboulos, A., and Prusiner, S.B. (1996). Subcellular colocalization of the cellular and scrapie prion proteins in caveolae-like membranous domains. Proc. Natl. Acad. Sci. USA *93*, 14945–14949.

Wang, F., Wang, X.H., Yuan, C.G., and Ma, J.Y. (2010). Generating a prion with bacterially expressed recombinant prion protein. Science *327*, 1132–1135.

Westaway, D., Zuliani, V., Cooper, C.M., Da Costa, M., Neuman, S., Jenny, A.L., Detwiler, L., and Prusiner, S.B. (1994). Homozygosity for prion protein alleles encoding glutamine-171 renders sheep susceptible to natural scrapie. Genes Dev. *8*, 959–969.

Yagi-Utsumi, M., Kameda, T., Yamaguchi, Y., and Kato, K. (2010). NMR characterization of the interactions between lyso-GM1 aqueous micelles and amyloid beta. FEBS Lett. *584*, 831–836.